ELSEVIER

www.elsevier.nl/locate/jorganchem

Journal of Organometallic Chemistry 597 (2000) 125–132

Journal of Organometallic Chemistry

Biscyclopentadienylzirconium(IV) η^3-propargyl/allenyl complexes

Patrick W. Blosser, Judith C. Gallucci, Andrew Wojcicki *

Department of Chemistry, The Ohio State University, Columbus, OH 43210, USA

Received 26 May 1999; received in revised form 28 September 1999

This paper is dedicated to Professor Stanisław Pasynkiewicz on the occasion of his 70th birthday.

Abstract

Reactions of each $Cp_2Zr(Me)Cl$ and Cp_2ZrCl_2 with $PhC{\equiv}CCH_2MgBr$ afford the η^3-propargyl/allenyl complexes $Cp_2Zr(Me)(\eta^3$-$CH_2CCPh)$ (**1**) and $Cp_2Zr(CH_2CCPh)_2$ (**2**), respectively. Both products were characterized by a combination of EI mass spectrometry and ^1H- and ^{13}C-NMR spectroscopy, and the structure of **1** was elucidated by a single-crystal X-ray analysis. Molecules of **1** contain an unsymmetrically ligated η^3-propargyl/allenyl group $C(1)H_2C(2)C(3)Ph$ with $Zr–C(1) = 2.658(4)$, $Zr–C(2) = 2.438(3)$ and $Zr–C(3) = 2.361(3)$ Å. Within the CH_2CCPh ligand, $C(1)–C(2) = 1.344(5)$, $C(2)–C(3) = 1.259(4)$ Å and $C(1)–C(2)–C(3) = 155.4(3)°$. The latter set of data indicates that a σ, π-allenyl resonance structure makes a relatively large contribution to the bonding description in **1** compared to a σ, π-propargyl resonance structure. The fragment $ZrC(10)C(1)C(2)C(3)$ ($C(10) = C$ of Me) is contained essentially in the mirror plane that reflects the two Cp rings. Complex **1** shows no fluxional behavior in its ^1H-NMR spectra over the temperature range 303–223 K. In contrast, **2** is fluxional, and its dynamic behavior persists on cooling even to 180 K. The ^1H-NMR spectra suggest that a rapid exchange of the modes of bonding of η^3-propargyl/allenyl and η^1-propargyl ligands may occur, with a probable participation of another $Zr–C_3H_2Ph$ bonding mode, possibly η^1-allenyl.

Keywords: Zirconium; Propargyl/allenyl complexes; Fluxional behavior; Crystal structure

---

1. Introduction

Following a report by Krivykh and co-workers [1] of the synthesis of the first transition-metal π- or η^3-propargyl/allenyl complexes[1], the number of such compounds has been steadily increasing [3,4]. Today well-characterized η^3-propargyl/allenyl complexes are known for several transition metals, including Mo [1], W [5], Re [5–7], Pd [8–10], Pt [9,11–14], Ti [15] and Zr [16,17]. Their chemistry has been explored in some detail for $[(PPh_3)_2M(\eta^3$-$CH_2CCR)]^+$ (M = Pt, Pd) [12,13,18], $[(\eta^5$-$C_5Me_5)Re(CO)_2(\eta^3$-$CH_2CCMe)]^+$ [6,7] and $[(\eta^6$-$C_6H_nMe_{6-n})Mo(CO)_2(\eta^3$-$CH_2CCH)]^+$ [1]. An important and unusual reaction of these cationic complexes is addition of nucleophilic reagents to the central carbon atom of the η^3-propargyl/allenyl ligand. η^3-Propargyl/allenyl complexes have been implicated as intermediates in organic synthesis [19].

Compared to Pt, Pd, Re and Mo, the early transition metals have not been explored much with respect to their propargyl/allenyl chemistry. A cationic complex $[(\eta^5$-$C_5Me_5)_2Zr(\eta^3$-$CH_2CCMe)]^+$ was obtained by treatment of $[(\eta^5$-$C_5Me_5)_2Zr(Me)(NMe_2Ph)][B(4$-$C_6H_4F)_4]$ with an excess of $MeC{\equiv}CMe$ [20]. It was assigned an η^3-CH_2CCMe structure on the basis of NMR spectroscopic data. In a similar study, the first step of the reactions of $(\eta^5$-$C_5Me_5)_2Ln(CH(SiMe_3)_2)$ (Ln = La, Ce) with $MeC{\equiv}CR$ (R = Me, Et, *n*-Pr) to give 1,2-disubstituted-3-alkylidenecyclobutanes was found to involve propargylic metalation to yield $(\eta^5$-$C_5Me_5)_2Ln(CH_2C{\equiv}CR)$ [21]. An analogous complex, $(\eta^5$-$C_5Me_5)_2Y(CH_2C{\equiv}CMe)$, was obtained from $(\eta^5$-$C_5Me_5)_2YH)_2$ and $MeC{\equiv}CMe$. NMR evidence supports a dynamic η^1-propargyl/η^1-allenyl or a static η^3-propargyl/allenyl structure of these organometallic species. More recently, another dynamic η^1-propargyl/

---

* Corresponding author: Fax: + 1-614-2921685.

E-mail address: wojcicki.1@osu.edu (A. Wojcicki)

[1] However, the synthesis of structurally related metal η^3-butenynyl (η^3-$C({=}CR_2)CCR$) complexes predated this discovery [2].

0022-328X/00/$ - see front matter
PII: S0022-328X(99)00655-5

η^1-allenyl complex, $CnY(Me)_2(C(Me)=C=CH_2)$ (Cn = 1,4,7-trimethyl-1,4,7-triazacyclononane), proposed to equilibrate via an η^3-propargyl/allenyl structure, was synthesized by Bercaw and co-workers [22]. Also, Rodriguez and Bazan [17] reported the synthesis of $(\eta^5\text{-}C_5Me_5)(TBM)Zr(\eta^3\text{-}CH_2CCMe)$ (TBM = tribenzylidenemethane), which was characterized by X-ray diffraction analysis. Finally, Ogoshi and Stryker [15] prepared the first titanium η^3-propargyl/allenyl complex $(\eta^5\text{-}C_5Me_5)_2Ti(\eta^3\text{-}CH_2CCPh)$ from $(\eta^5\text{-}C_5Me_5)_2$-TiCl and $PhC{\equiv}CCH_2Br$ in the presence of SmI_2.

Organozirconium compounds have been investigated intensively in synthesis, both as stoichiometric reagents and as catalysts [23]. In that general vein, we set out to prepare biscyclopentadienylzirconium(IV) η^3-propargyl/allenyl complexes by utilizing reactions of the corresponding biscyclopentadienylzirconium(IV) halides with Grignard reagents. Reported herein are the syntheses of $Cp_2Zr(Me)(\eta^3\text{-}CH_2CCPh)$ (**1**), the structure of which was elucidated by X-ray diffraction analysis, and of fluxional $Cp_2Zr(CH_2CCPh)_2$ (**2**). This study was communicated in a preliminary form [16].

2. Experimental

2.1. General procedures

All reactions and manipulations were conducted under an atmosphere of Ar by use of standard procedures [24]. Solvents were dried, distilled under an Ar atmosphere and degassed before use [25]. ^1H- and ^{13}C-NMR spectra were recorded on a Bruker AM-300 spectrometer, and the chemical shifts are given in ppm downfield from Me_4Si. Infrared spectra were obtained on a Perkin–Elmer model 283B spectrophotometer and were calibrated with polystyrene. EI mass spectra were recorded on a Kratos VG70-250S spectrometer by Mr David C. Chang.

Reagents were obtained from various commercial sources and used as received. Literature procedures were followed to synthesize $Cp_2Zr(Me)Cl$ [26] and $PhC{\equiv}CCH_2Br$ [27]. The latter was used to make $PhC{\equiv}CCH_2MgBr$ in a continuous Grignard apparatus [28].

2.2. Preparation of $Cp_2Zr(Me)(\eta^3\text{-}CH_2CCPh)$ (1)

A solution of $PhC{\equiv}CCH_2MgBr$ (25.4 mmol, determined by titration) in diethyl ether (70 ml) was added dropwise over 2 h to a stirred solution of $Cp_2Zr(Me)Cl$ (4.96 g, 18.2 mmol) in diethyl ether (150 ml) at 0°C. After the addition was complete, the reaction mixture was warmed to room temperature (r.t.) and stirred for an additional 3 h. All volatiles were then removed under reduced pressure, and hexane (100 ml) was added to the residue. After 2 h of vigorous stirring, the hexane extract was filtered and concentrated to ca. 10 ml to yield a precipitate. The solid remaining on the filter frit was extracted successively with 100, 300 and 300 ml of hexane, and the extracts were similarly concentrated to furnish additional product. The precipitates were dried under vacuum for 48 h to give an air-sensitive tan solid. Total yield, 6.29 g (98%). **1**: IR (KBr): 2176 (m), 1924 (m) cm^{-1}. ^1H-NMR (300 K, CD_2Cl_2): 7.67–7.37 (m, 5H, Ph), 5.64 (s, 10H, 2Cp), 3.37 (s, 2H, CH_2), 0.34 (s, 3H, Me). $^{13}C\{^1H\}$-NMR (300 K, CD_2Cl_2): 133–127 (Ph), 120.5 and 114.1 (2s, Ph*C* and PhC*C*), 107.2 (s, Cp), 55.5 (s, CH_2), 4.8 (s, Me). ^{13}C-NMR (300 K, CD_2Cl_2): 55.5 (t, $^1J_{CH} = 167$ Hz), 4.8 (q, $^1J_{CH} = 123$ Hz). EI-MS, ^{90}Zr, m/z (ion, relative intensity) 350.060 (exact M^+, 0.7; $C_{20}H_{20}Zr$ calc. 350.061), 335 (M^+–Me, 73), 220 (M^+–Me–C_3H_2Ph, 52), 115 ($C_3H_2Ph^+$, 100).

2.3. Preparation of $Cp_2Zr(CH_2CCPh)_2$ (2)

A solution of $PhC{\equiv}CCH_2MgBr$ (19.1 mmol, determined by titration) in diethyl ether (60 ml) was added dropwise over 2 h to a stirred solution of Cp_2ZrCl_2 (2.07 g, 7.08 mmol) in CH_2Cl_2 (75 ml) at 0°C. The reaction mixture was then warmed to r.t. and stirred for an additional 3 h. Volatile matter was removed under reduced pressure, toluene (100 ml) was added to the residue, and the contents were vigorously stirred for 3 h. The mixture was filtered, and the solid collected on a frit was further extracted with toluene (50 ml). The toluene extracts were combined, solvent was removed, and the deep red oily residue was dried under vacuum for 5 days to give a brittle, glassy solid (2.37 g, 74% yield). This crude product can be purified by extraction into hexane, filtration, and cooling of the filtrate at −78°C for 5 h to induce formation of an air-sensitive brown–red powder. Yield, ca. 0.40 g per 1.0 g of crude product. **2**: ^1H-NMR (300 K, CD_2Cl_2): 7.58–7.30 (m, 10H, 2Ph), 5.80 (s, 10H, 2Cp), 2.80 (s, 4H, $2CH_2$). $^{13}C\{^1H\}$-NMR (300 K, CD_2Cl_2): 132–127 (Ph), 112.9 and 98.8 (2s, Ph*C* and PhC*C*), 108.0 (s, Cp), 30.7 (s, CH_2). ^{13}C-NMR (300 K, CD_2Cl_2): 30.7 (t, $^1J_{CH} = 151$ Hz). EI-MS, ^{90}Zr, m/z (ion, relative intensity) 450.093 (exact M^+, 8.8; $C_{28}H_{24}Zr$ calc. 450.093), 335 (M^+–C_3H_2Ph, 74), 220 (M^+–$2C_3H_2Ph$, 100), 115 ($C_3H_2Ph^+$, 59).

2.4. Crystallographic analysis of $Cp_2Zr(Me)(\eta^3\text{-}CH_2CCPh)$ (1)

Crystals of **1** were grown from diethyl ether–THF; a colorless cube was mounted in an argon-filled glass capillary. Examination of the diffraction pattern on a Rigaku AFC5S diffractometer indicated a monoclinic crystal system with systematic absences $h0l$, $l = 2n + 1$

and $0k0$, $k = 2n+1$. The space group is uniquely determined as $P2_1/c$. The cell constants are based on a symmetry-restricted least-squares fit of the diffractometer setting angles for 25 reflections in the 2θ range 23–30° with Mo–K$_\alpha$ radiation ($\lambda(\mathrm{K}_{\bar{\alpha}}) = 0.71073$ Å).

During the course of data collection, six standard reflections were measured after every 150 reflections and they all showed a steady decrease in intensity. A linear decay correction was applied to the data based on an average decrease of 13.2% in intensity. No correction for absorption was made.

The position of the Zr atom was located on a Patterson map and then used as a phasing model in DIRDIF [29]. The rest of the molecule appeared cleanly in the resultant electron density map. All full-matrix least-squares refinements were done on F with the TEXSAN package [30]. After a cycle of anisotropic refinement, the hydrogen atoms on the phenyl and Cp rings were included in the model as fixed contributions at their calculated positions with C–H = 0.98 Å and $B_\mathrm{H} = 1.2B\mathrm{eq}$ (attached carbon atom). The hydrogen atoms bonded to C(1) and C(10) were included initially in the model as fixed contributions at their positions from a difference electron density map. They were subsequently refined isotropically. In the latter stages of refinement, a secondary extinction coefficient was introduced [31] and refined to $2.6(1) \times 10^{-6}$. The final refinement cycle was based on 2692 intensities with $F_\mathrm{o}^2 > 3\sigma(F_\mathrm{o}^2)$ and 211 variables and resulted in agreement factors of $R = 0.029$ and $R_w = 0.035$. The maximum and minimum peak heights in the final difference electron density map are 0.39 and -0.42 e Å^{-3}. Scattering factors for the non-hydrogen atoms, including terms for anomalous dispersion [32], and the scattering factor for the hydrogen atom [33] are from the literature. A summary of the crystal data and the details of the intensity data collection and refinement are provided in Table 1.

Table 1
Crystal data and experimental details for $Cp_2Zr(Me)(\eta^3\text{-}CH_2CCPh)$ (**1**)

Formula	$C_{20}H_{20}Zr$
Formula weight	351.60
Space group	$P2_1/c$
a (Å)	8.147(2)
b (Å)	8.766(2)
c (Å)	22.672(3)
β (°)	97.10(2)
V (Å^3)	1607(1)
Z	4
$D_\mathrm{calc.}$ (g cm^{-3})	1.45
Crystal size (mm)	$0.31 \times 0.35 \times 0.38$
Radiation	Mo–K$_\alpha$ with graphite monochromator
Linear absorption coefficient (cm^{-1})	6.63
Temperature (K)	296
2θ limits (°)	$4 \leq 2\theta \leq 55$
Scan speed (deg min^{-1} in ω)	4, with a maximum of four scans per reflection
Background time/scan time	0.5
Scan range (deg in ω)	$1.00 + 0.35 \tan\theta$
Scan type	ω
Data collected	$+h, +k, \pm l$
No. of unique data	3945
No. of unique data with $F_\mathrm{o}^2 > 3\sigma(F_\mathrm{o}^2)$	2692
Final no. of variables	211
$R(F)$ [a]	0.029
$R_\mathrm{w}(F)$ [b]	0.035
Error in observation of unit wt (e)	1.30

[a] $R(F) = \Sigma||F_\mathrm{o}| - |F_\mathrm{c}||/\Sigma|F_\mathrm{o}|$.

[b] $R_\mathrm{w}(F) = [\Sigma\, w(|F_\mathrm{o}| - |F_\mathrm{c}|)^2/\Sigma\, w|F_\mathrm{o}|^2]^{1/2}$ with $w = 1/\sigma^2(F_\mathrm{o})$.

3. Results and discussion

3.1. Synthesis of $Cp_2Zr(Me)(\eta^3\text{-}CH_2CCPh)$ (**1**) and $Cp_2Zr(CH_2CCPH)_2$ (**2**)

Complexes **1** and **2** were obtained by treatment of the appropriate zirconium(IV) chloride precursors with the Grignard reagent $PhC{\equiv}CCH_2MgBr$. Specifically, **1** resulted from reaction of $Cp_2Zr(Me)Cl$ with an excess (ca. 1.4 equivalents) of $PhC{\equiv}CCH_2MgBr$ in diethyl ether at 0–25°C and was isolated by the extraction of the non-volatile residue from the reaction mixture into hexane followed by crystallization. Complex **2** formed upon addition of ca. 2.7 equivalents of the Grignard reagent to Cp_2ZrCl_2 in CH_2Cl_2 at 0°C with warming to 25°C. Its isolation–purification workup consisted of the extraction of the non-volatile residue from the reaction mixture into toluene, another extraction of the evaporated toluene fraction into hexane, and crystallization. This procedure, described in more detail in Section 2, effectively removed magnesium salts and organic side products from both **1** and **2**. Special care must be exercised in the preparation of the Grignard reagent [28], which shows considerable propensity to coupling of the phenylpropargyl groups [34].

Complex **1** was isolated in 98% yield as a tan solid. The yield of **2**, a red–brown solid, depends on the degree of purity desired, and is typically within 30–74%. Both complexes are very air sensitive and show insufficient stability for commercial elemental analysis. Their purity and chemical composition were ascertained by ^{1}H- and ^{13}C-NMR spectroscopy (vide infra) and EI mass spectrometry. The mass spectrum of **1** revealed an exact molecular mass of 350.060 (calc. 350.061) and showed stepwise loss of the methyl and phenylpropargyl ligands. For **2**, an exact molecular mass of 450.93 was obtained (calc. 450.93), and the molecular ion underwent fragmentation by consecutive loss of the two C_3H_2Ph groups.

Table 2
Selected ^{1}H- and ^{13}C-NMR data for transition-metal η^{3}-phenylpropargyl/phenylallenyl and various zirconium η^{3}-propargyl/allenyl complexes [a]

Complex	δ, ^{1}H-NMR	δ, ^{13}C-NMR ($^{1}J_{CH}$)		Reference
	CH_2	CC	CH_2	
$[(PPh_3)_2Pt(\eta^3\text{-}CH_2CCPh)]O_3SCF_3$	2.74	102.1, 97.3	48.3(170)	[9]
$[PPh_3)_2Pd(\eta^3\text{-}CH_2CCPh)]BF_4$	3.19	105.4, 94.2	50.9	[9]
$Cp_2Zr(Me)(\eta^3\text{-}CH_2CCPh)$ (**1**)	3.37	120.5, 114.1	55.5(167)	This work
$Cp_2Zr(CH_2CCPh)_2$ (**2**)	2.80	112.9, 98.8	30.7(151)	This work
$(\eta^5\text{-}C_5Me_5)(TBM)Zr(\eta^3\text{-}CH_2CCMe)$	2.51, 2.30	99.9, 91.7	51.0	[17]
$[(\eta^5\text{-}C_5Me_5)_2Zr(CH_2CCMe)][B(4\text{-}C_6H_4F)_4]$ [b]	2.93	128.4, 103.5	61.7(158)	[20]

[a] At ambient temperature except as noted. δ in ppm, J in Hz.
[b] ^{13}C-NMR at 243 K.

3.2. Spectroscopic properties of $Cp_2Zr(Me)(\eta^3\text{-}CH_2\text{-}CCPh)$ (*1*) and $Cp_2Zr(CH_2CCPh)_2$ (*2*)

The ^{1}H- and ^{13}C-NMR spectra of **1** are compatible with a structure containing η^{3} ligated propargyl/allenyl. Thus, the proton CH_2 signal at δ 3.37 is close to that observed for other transition-metal complexes containing an η^{3}-phenylpropargyl group (cf. Table 2). However, it is at a somewhat lower field compared to the corresponding signal of η^{1}-phenylpropargyl complexes, which resonate at $\delta < 2.6$ [9,35–37].

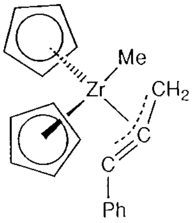

1

The ^{13}C-NMR spectrum provides further evidence for η^{3}-CH_2CCPh ligation, but is not entirely consistent with the two η^{1} modes of bonding of this group. Accordingly, the resonances of the *C*Ph and *C*CH_2 carbons observed at δ 120.5 and 114.1 are in the normal region for either η^{3}-CH_2CCPh or η^{1}-$CH_2C{\equiv}CPh$ [9,36,37]. However, η^{1}-allenyl bonding, $MC(Ph){=}C{=}CH_2$, would have resulted in a =C= signal at δ ca. 200 [37], and such a low-field signal is absent in the spectrum. Furthermore, the position of the CH_2 resonance at δ 55.5 is in accord with the presence of either η^{3}-CH_2CCPh or η^{1}-$C(Ph){=}C{=}CH_2$, but rules out η^{1}-$CH_2C{\equiv}CPh$, which shows this signal at $\delta \leq 0$ [9,36,37].

The magnitude of the one-bond coupling constant $^{1}J_{CH}$ for the CH_2 group supports these generalizations. The value of 167 Hz indicates sp^{2} hybridization at carbon and points to either η^{3}-CH_2CCPh or η^{1}-$C(Ph){=}C{=}CH_2$ ligation (Table 2). Furthermore, it rules out η^{1}-$CH_2C{\equiv}CPh$, which shows a $^{1}J_{CH}$ of 135–145 Hz [9,37], consistent with sp^{3} hybridization at the CH_2 carbon.

There is no indication of fluxional behavior of **1** from its ^{1}H-NMR spectra, which remain unchanged over the temperature range 303–223 K.

The ambient temperature (300 K) ^{1}H- and ^{13}C-NMR spectra of **2** shows that the two CH_2CCPh ligands are equivalent. Sharp signals of the appropriate nuclei are observed at δ 2.80 (^{1}H CH_2), 112.9 and 98.8 (^{13}C CC) and 30.7 (^{13}C CH_2). These chemical shifts are on the high-field side of the typical ones for η^{3}-CH_2CCPh. Likewise, the $^{1}J_{CH}$ coupling constant associated with the CH_2 group is only 151 Hz, a value between that expected for sp^{2} and sp^{3} hybridization at that carbon. Because of these apparent anomalies, we examined ^{1}H-NMR spectra of **2** in CD_2Cl_2 solution over the temperature range 300–180 K. As shown in Fig. 1, lowering the temperature to 240 K causes the CH_2 signal at δ 2.80 to broaden while the signals of the Ph and Cp protons remain essentially unchanged. At 180 K, the original CH_2 signal is no longer discernible; instead two very broad resonances centered approximately at δ 3.3 and 1.9 are present. Satisfactory spectra could not be obtained below 180 K. All of the above changes can be reversed upon warming the sample.

It is tempting to offer an explanation of the aforementioned dynamic behavior of **2** in terms of rapid exchange of the modes of bonding of the η^{3}-propargyl/allenyl and η^{1}-propargyl ligands as shown below. Such a ligand interchange is supported by the positions of the broad CH_2 proton resonances at ca. δ 3.3 and 1.9 in the 180 K spectrum. However, it would be presumptuous to draw conclusions from these limited data, especially since fluxional behavior is still ongoing at that temperature. Furthermore, the higher temperature signal at δ 2.8 does not represent the weighted average of the resonance positions at δ 3.3 and 1.9, if the only organozirconium species present is $Cp_2Zr(\eta^1\text{-}CH_2C{\equiv}CPh)(\eta^3\text{-}CH_2CCPh)$. Therefore, another species resonating at ca. δ 3.3, possibly $Cp_2Zr(\eta^1\text{-}C(Ph){=}C{=}CH_2)(\eta^3\text{-}CH_2CCPh)$, also seems likely to be involved in the fluxional process. Both $Cp_2Zr(\eta^1\text{-}CH_2C{\equiv}CPh)(\eta^3\text{-}CH_2CCPh)$ and $Cp_2Zr(\eta^1\text{-}C(Ph){=}C{=}CH_2)(\eta^3\text{-}CH_2CCPh)$ obey the 18-electron rule and would be analogous to the methyl η^3-propargyl/allenyl complex **1** in terms of ligand hapticity.

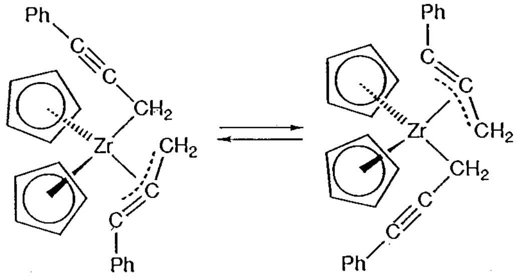

2

Complex **2** represents the first example of a transition-metal compound containing propargyl/allenyl ligands that are bonded differently to a metal center. Similarly constituted metal allyl complexes are known [38–41] and include $Cp_2Zr(\eta^1\text{-}CH_2C(R){=}CH_2)(\eta^3\text{-}CH_2C(R)CH_2)$ ($R = H$, Me) [39] and $CpZr(\eta^1\text{-}CH_2CH{=}CH_2)(\eta^3\text{-}CH_2CHCH_2)_2$ [41]. Some of them, including the listed zirconium complexes, exhibit fluxional behavior that exchanges the η^1 and η^3 modes of bonding of the allyl groups.

3.3. Structural characterization of $Cp_2Zr(Me)(\eta^3\text{-}CH_2CCPh)$ (**1**)

The molecular structure of **1** with atom-numbering scheme is presented as Fig. 2, whereas selected bond distances, bond angles and dihedral angles are given in Table 3. Molecules of **1** are comprised of a Zr center, two Cp rings, one propargyl/allenyl ligand and one methyl ligand. Both Cp groups are η^5 bonded to Zr and tilted, the dihedral angle between the two planar rings being 52.4(3)°. The Zr–(Cp ring centroid) distances measure 2.237(4) and 2.234(5) Å, and are essentially equal to the values reported for Cp_2ZrMe_2 (2.23 Å), $(Cp_2ZrMe)_2O$ (2.24 Å) and $Cp_2Zr(Me)Cl$ (2.21 and 2.24 Å) [42]. The Zr–C(Cp) bond lengths fall in the range 2.508(3)–2.550(4) Å (2.528(4) Å average) and compare well with those published for other biscyclopentadienylzirconium(IV) complexes [42,43].

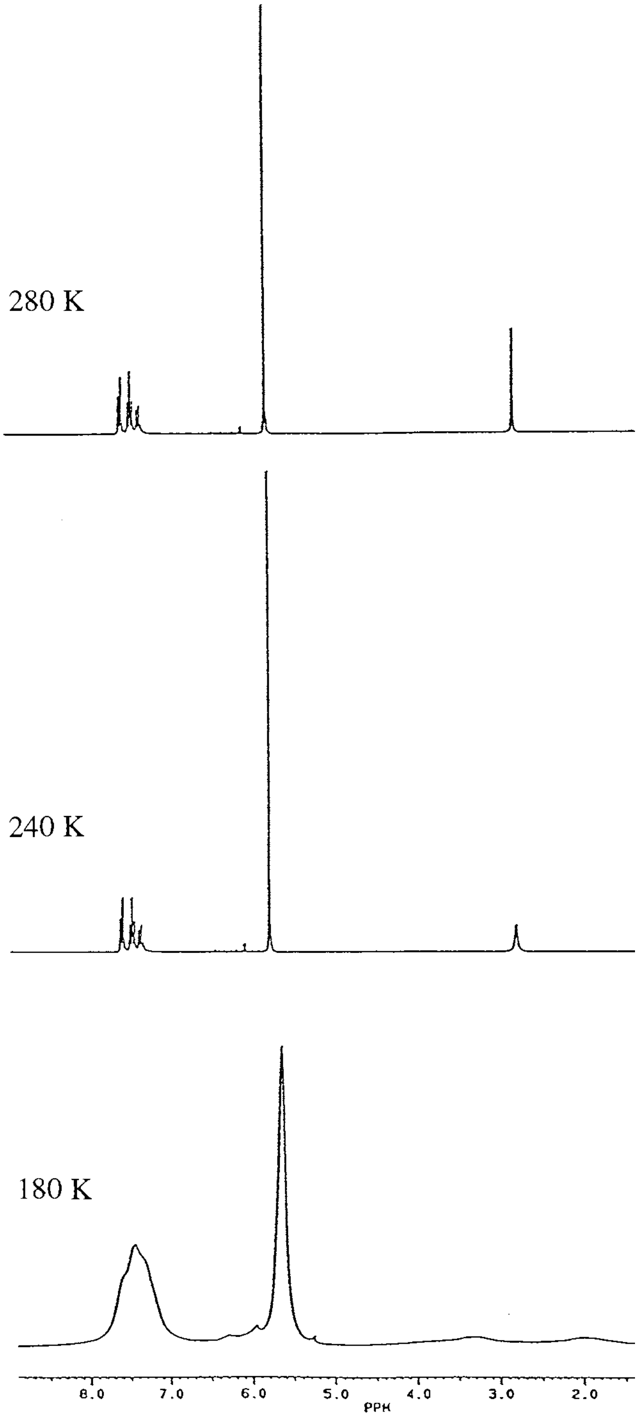

Fig. 1. ^1H-NMR spectra of **2** in CD_2Cl_2 solution in the temperature range 300–180 K.

The C_3 backbone of the propargyl/allenyl ligand (i.e. C(1)C(2)C(3)) is virtually coplanar with Zr (atom displacements from the least-squares plane: Zr 0.000, C(1) 0.006, C(2) 0.005 and C(3) 0.003 Å). Such a coplanar arrangement of the C_3 and M was noted earlier [1,9,10] and appears to be a characteristic structural feature of transition-metal η^3-propargyl/allenyl complexes. A recent theoretical paper addresses this subject [44]. The carbon atom of the methyl ligand (C(10)) is essentially in the ZrC(1)C(2)C(3) plane (0.103(4) Å displacement) and 2.364(4) Å away from Zr. The Zr–C(10) bond length may be compared with the Zr–Me bond distances in some related compounds: 2.280(5) and 2.273(5) Å in Cp_2ZrMe_2, 2.276(9) Å in $(Cp_2ZrMe)_2O$ and 2.35(1) and 2.36(2) Å in $Cp_2Zr(Me)Cl$ [42]. The atoms Zr, C(1), C(2), C(3) and C(10) all lie in the mirror plane that reflects the two Cp groups of Cp_2Zr; this perspective of the molecule of **1** is shown in Fig. 3. As a result of this symmetry, the two hydrogens bonded

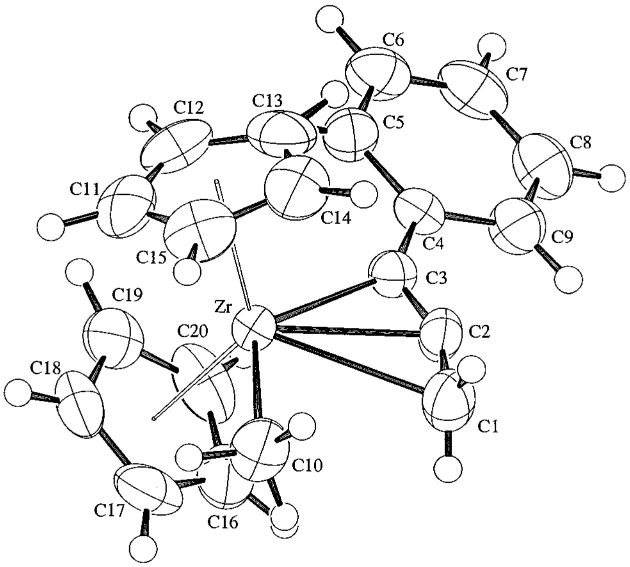

Fig. 2. ORTEP plot of **1** with atom-numbering scheme. The non-hydrogen atoms are represented by 50% probability thermal ellipsoids whereas the hydrogen atoms are drawn with an artificial radius.

to C(1) are magnetically equivalent in the ^{1}H-NMR spectrum of **1** (vide supra).

We now come to the most interesting part of the structure, namely, the propargyl/allenyl ligand and its attachment to the zirconium center. The propargyl/allenyl bond lengths C(1)–C(2) and C(2)–C(3) are 1.344(5) and 1.259(4) Å, respectively, while the bond angle C(1)–C(2)–C(3) measures 155.4(3)°. The bonding of this ligand to Zr is characterized by the distances Zr–C(1) = 2.658(4), Zr–C(2) = 2.438(3) and Zr–C(3) = 2.361(3) Å. The corresponding bond lengths and angles in other structurally investigated metal η^3-propargyl/allenyl complexes [1,9,10,14,17] are listed for comparison in Table 4.

A comparison of the data reveals that the C–CH$_2$ distance in **1** (i.e. C(1)–C(2)) is relatively short while the C–CPh distance in **1** (i.e. C(2)–C(3)) is relatively long. In fact, the difference between the two C–C bond lengths in **1** is only 0.085 Å, compared to 0.124–0.168 Å (0.145 Å average) in the other, non-zirconium complexes. If we consider the two resonance structures **I** and **II** that contribute to the bonding description of metal η^3-propargyl/allenyl complexes, then the small difference between the C–C bond lengths in **1** suggests that the allenyl representation (**II**) is relatively more important than the propargyl representation (**I**).

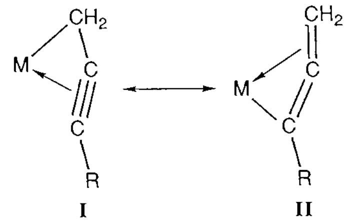

The attachment of the propargyl/allenyl ligand to zirconium is also characterized by unusual features. The Zr–C bond distances increase substantially on going from Zr–C(3) to Zr–C(2) and to Zr–C(1). The last Zr–C bond is exceptionally long at 2.658(4) Å and indicates a significant distortion from the usual metal–η^3-propargyl/allenyl interaction. This distortion is accompanied

Table 3
Selected bond distances (Å), bond angles (°) and dihedral angles (°) for Cp$_2$Zr(Me)(η^3-CH$_2$CCPh) (**1**)

Bond distances			
Zr–C(1)	2.658(4)	Zr–C(16)	2.541(4)
Zr–C(2)	2.438(3)	Zr–C(17)	2.541(3)
Zr–C(3)	2.361(3)	Zr–C(18)	2.517(3)
Zr–C(10)	2.364(4)	Zr–C(19)	2.508(3)
Zr–C(11)	2.514(3)	Zr–C(20)	2.522(3)
Zr–C(12)	2.517(3)	C(1)–C(2)	1.344(5)
Zr–C(13)	2.550(4)	C(2)–C(3)	1.259(4)
Zr–C(14)	2.537(3)	C(3)–C(4)	1.462(4)
Zr–C(15)	2.533(3)		
Bond angles			
C(1)–Zr–C(2)	30.2(1)	Zr–C(1)–C(2)	65.8(2)
C(1)–Zr–C(10)	68.0(1)	Zr–C(2)–C(3)	71.4(2)
C(2)–Zr–C(3)	30.4(1)	Zr–C(3)–C(4)	144.4(2)
C(2)–Zr–C(10)	98.2(1)	C(1)–C(2)–C(3)	155.4(3)
C(3)–Zr–C(10)	128.5(1)	C(2)–C(3)–C(4)	137.3(3)
Dihedral angles			
C(1)C(2)C(3), C(1)C(2)Zr	1.87		
C(1)C(2)C(3), C(2)C(3)Zr	1.96		
C(1)C(2)Zr, C(2)C(3)Zr	0.82		
C(1)C(2)C(3)Zr, C(11)C(12)C(13)C(14)C(15)	24.6(2)		
C(1)C(2)C(3)Zr, C(16)C(17)C(18)C(19)C(20)	28.0(2)		

Table 4
Selected bond distances (Å) and angles (°) in metal η^3-propargyl/allenyl complexes

Complex	Bond distance					Bond angle	Reference
	C–CH_2	C–CR	M–CH_2	M–C	M–CR	CH_2–C–CR	
$[(\eta^6\text{-}C_6HMe_5)Mo(CO)_2(\eta^3\text{-}CH_2CCH)]BF_4$	1.380(4)	1.236(4)	2.340(3)	2.282(3)	2.319(3)	150.9(3)	[1]
$[(PPh_3)_2Pt(\eta^3\text{-}CH_2CCPh)]O_3SCF_3$	1.395(14)	1.227(13)	2.186(11)	2.150(8)	2.273(9)	152.2(9)	[9]
$[(PPh_3)_2Pd(\eta^3\text{-}CH_2CCPh)]BF_4$	1.385(7)	1.233(7)	2.162(5)	2.143(4)	2.334(5)	154.7(5)	[9]
$(PPh_3)(C_6F_5)Pd(\eta^3\text{-}CH_2CCBu\text{-}t)$	1.38(1)	1.244(9)	2.156(7)	2.116(6)	2.238(7)	151.6(7)	[10]
$[(PPh_3)_2Pt(\eta^3\text{-}CH(Me)CCBu\text{-}t)]O_3SCF_3$	1.390(5)	1.266(5)	2.243(3)	2.140(3)	2.265(3)	154.1(3)	[14]
$Cp_2Zr(Me)(\eta^3\text{-}CH_2CCPh)$ (**1**)	1.344(5)	1.259(4)	2.658(4)	2.438(3)	2.361(3)	155.4(3)	This work
$(\eta^5\text{-}C_5Me_5)(TBM)Zr(\eta^3\text{-}CH_2CCMe)$	1.376(7)	1.218(7)	2.498(5)	2.408(4)	2.444(5)	Essentially linear	[17]

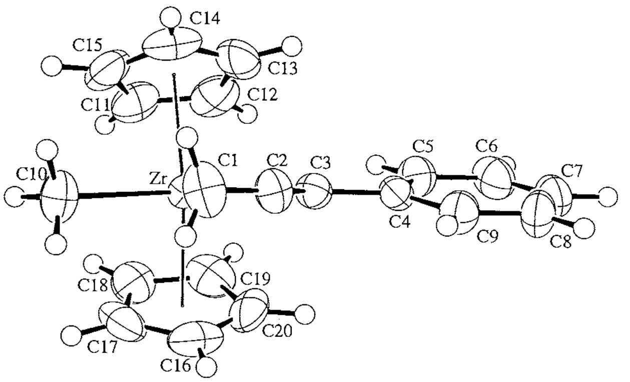

Fig. 3. Molecular structure of **1** showing the essentially planar ZrC(1)C(2)C(3)C(10) fragment.

by a somewhat lesser than normal (cf. Table 4) degree of bending of the propargyl/allenyl fragment on coordination (C(1)–C(2)–C(3) = 155.4(3)°).

There are literature reports of similar unusual structural features in organozirconium compounds. A dizirconium allenediyl complex, $(Cp_2ZrEt)_2(\mu_2\text{-}\eta^1\text{:}\eta^2\text{-}CCCMe_2)$ (**III**), shows a marked resemblance to **1** if the σ-bonded Cp_2ZrEt group is replaced with a Ph group. For example, in **III**, the Zr–C distances are, from left to right in $Me_2CC{\equiv}C$, 2.819(5), 2.420(4) and 2.433(4) Å, while the C–C bond distances are 1.352(6) and 1.256(5) Å [45]. However, even a more striking bonding analogy exists between **1** and the allyl complex $CpZr(\eta^1\text{–}CH_2\text{-}CH{=}CH_2)(\eta^3\text{-}CH_2CHCH_2)_2$ [41]. The latter contains two differently bonded η^3-allyl ligands, with one of them being unsymmetrically attached to zirconium (Zr–C(1) = 2.442(4), Zr–C(2) = 2.523(3), Zr–C(3) = 2.624(3) Å; also, C(1)–C(2) = 1.412(5), C(2)–C(3) = 1.371(6) Å). The aforementioned metrical data suggest a σ, π-type metal–η^3-allyl interaction that might represent an intermediate structural position during η^3 to η^1 interconversion of metal allyls. It is possible that the distortions in ligation of $\eta^3\text{-}CH_2CHCH_2$ and $\eta^3\text{-}CH_2CCPh$ to Zr observed in $CpZr(\eta^1\text{-}CH_2CH{=}CH_2)(\eta^3\text{-}CH_2CHCH_2)_2$ and **1**, respectively, are of a similar type. In other words, the zirconium–propargyl/allenyl interaction in **1** may be representative of a structural situation that is intermediate between π-propargyl/allenyl and σ-allenyl bonding.

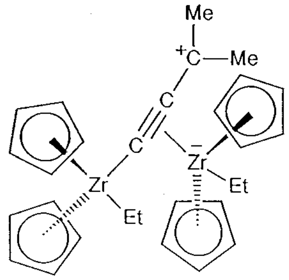

III

4. Supplementary material

Crystallographic data for the structural analysis have been deposited with the Cambridge Crystallographic Data Centre, CCDC no. 133862 for compound **1**. Copies of this information may be obtained free of charge from The Director, CCDC, 12, Union Road, Cambridge CB2 1EZ, UK. Fax: +44-1223-336033; e-mail: deposit@ccdc.cam.ac.uk or http://www.ccdc.cam.ac.uk.

Acknowledgements

This study was supported by The Ohio State University. P.W.B. thanks the Procter and Gamble Co. for a graduate fellowship.

References

[1] V.V. Krivykh, E.S. Taits, P.V. Petrovskii, Yu. T. Struchkov, A.I. Yanovskii, Mendeleev Commun. (1991) 103.
[2] J. Gotzig, H. Otto, H. Werner, J. Organomet. Chem. 287 (1985) 247.
[3] A. Wojcicki, New J. Chem. 18 (1994) 61.
[4] S. Doherty, J.F. Corrigan, A.J. Carty, E. Sappa, Adv. Organomet. Chem. 37 (1995) 39.

[5] (a) V.V. Krivykh, Organomet. Chem. USSR (Engl. Transl.) 5 (1992) 113. (b) V.V. Krivykh, Metallorg. Khim. 5 (1992) 213.
[6] C.P. Casey, C.S. Yi, J. Am. Chem. Soc. 114 (1992) 6597.
[7] C.P. Casey, J.R. Nash, C.S. Yi, A.D. Selmeczy, S. Chung, D.R. Powell, R.K. Hayashi, J. Am. Chem. Soc. 120 (1998) 722.
[8] S. Ogoshi, K. Tsutsumi, H. Kurosawa, J. Organomet. Chem. 493 (1995) C19.
[9] M.W. Baize, P.W. Blosser, V. Plantevin, D.G. Schimpff, J.C. Gallucci, A. Wojcicki, Organometallics 15 (1996) 164.
[10] K. Tsutsumi, S. Ogoshi, S. Nishiguchi, H. Kurosawa, J. Am. Chem. Soc. 120 (1998) 1938.
[11] T.-M. Huang, J.-T. Chen, G.-H. Lee, Y. Wang, J. Am. Chem. Soc. 115 (1993) 1170.
[12] P.W. Blosser, D.G. Schimpff, J.C. Gallucci, A. Wojcicki, Organometallics 12 (1993) 1993.
[13] T.-M. Huang, R.-H. Hsu, C.-S. Yang, J.-T. Chen, G.-H. Lee, Y. Wang, Organometallics 13 (1994) 3657.
[14] P.J. Stang, C.M. Crittell, A.M. Arif, Organometallics 12 (1993) 4799.
[15] S. Ogoshi, J.M. Stryker, J. Am. Chem. Soc. 120 (1998) 3514.
[16] P.W. Blosser, J.C. Gallucci, A. Wojcicki, J. Am. Chem. Soc. 115 (1993) 2994.
[17] G. Rodriguez, G.C. Bazan, J. Am. Chem. Soc. 119 (1997) 343.
[18] J.-T. Chen, R.-H. Hsu, A.J. Chen, J. Am. Chem. Soc. 120 (1998) 3243 and references therein.
[19] J. Tsuji, T. Mandai, Angew. Chem. Int. Ed. Engl. 34 (1995) 2589.
[20] A.D. Horton, A.G. Orpen, Organometallics 11 (1992) 8.
[21] H.J. Heeres, A. Heeres, J.H. Teuben, Organometallics 9 (1990) 1508.
[22] S. Hajela, W.P. Schaefer, J.E. Bercaw, J. Organomet. Chem. 532 (1997) 45.
[23] E.W. Abel, F.G.A. Stone, G. Wilkinson (Eds.), Comprehensive Organometallic Chemistry II, vol. 12, Pergamon, Oxford, 1995.
[24] D.F. Shriver, M.A. Drezdzon, The Manipulation of Air-Sensitive Compounds, second ed., Wiley, New York, 1986.
[25] D.D. Perrin, W.L.F. Armarego, D.R. Perrin, Purification of Laboratory Chemicals, Pergamon, Oxford, 1966.
[26] P.C. Wailes, H. Weigold, A.P. Bell, J. Organomet. Chem. 33 (1971) 181.
[27] L. Brandsma, H.D. Verkruijsse, Synthesis of Acetylenes, Allenes, and Cumulenes, Elsevier, New York, 1981, p. 219.
[28] D.C. Rowland, M.Sc. Thesis, The Ohio State University, 1948.
[29] V. Parthasarathi, P.T. Beurskens, H.J.B. Slot, Acta Crystallogr. A39 (1983) 860.
[30] TEXSAN, Single Crystal Structure Analysis Software, Version 5.0, Molecular Structure Corp., The Woodlands, TX 77381, 1989.
[31] W.M. Zachariasen, Acta Crystallogr. 16 (1963) 1139.
[32] International Tables of X-ray Crystallography, vol. IV, Kynoch, Birmingham, 1974, pp. 71 and 148.
[33] R.F. Stewart, E.R. Davidson, W.T. Simpson, J. Chem. Phys. 42 (1965) 3175.
[34] M.S. Kharash, O. Reinmuth (Eds.), Grignard Reactions of Nonmetallic Substances, Prentice-Hall, New York, 1954, Chapter 1.
[35] J.O. Kroll, A. Wojcicki, J. Organomet. Chem. 66 (1974) 95.
[36] F. Ungváry, A. Wojcicki, J. Organomet. Chem. 396 (1990) 95.
[37] C.E. Shuchart, R.R. Willis, A. Wojcicki, J. Organomet. Chem. 424 (1992) 185 and references therein.
[38] J. Powell, B.L. Shaw, J. Chem. Soc. A (1968) 583.
[39] H.A. Martin, P.J. Lamaire, F. Jellinek, J. Organomet. Chem. 14 (1968) 149.
[40] B. Henc, P.W. Jolly, R. Salz, S. Stobbe, G. Wilke, R. Benn, R. Mynott, K. Seevogel, R. Goddard, C. Krüger, J. Organomet. Chem. 191 (1980) 449.
[41] G. Erker, K. Berg, K. Angermund, C. Krüger, Organometallics 6 (1987) 2620.
[42] W.E. Hunter, D.C. Hrncir, R. Vann Bynum, R.A. Penttila, J.L. Atwood, Organometallics 2 (1983) 750.
[43] W.E. Hunter, J.L. Atwood, G. Fachinetti, C. Floriani, J. Organomet. Chem. 204 (1981) 67.
[44] J.P. Graham, A. Wojcicki, B.E. Bursten, Organometallics 18 (1999) 837.
[45] P. Binger, F. Langhauser, B. Gabor, R. Mynott, A.T. Herrmann, C. Krüger, J. Chem. Soc. Chem. Commun. (1992) 505.